The Kuiper Belt Explored by Serendipitous Stellar Occultations

F. Roques
Paris Observatory

G. Georgevits
University of New South Wales

A. Doressoundiram
Paris Observatory

The possibility of exploring the Kuiper belt by searching for fortuitous stellar occultations has been under development for several years. This technique has the potential to permit exploration of the Kuiper belt down to objects of subkilometer radius. High-speed photometric observations provide lightcurves in which the occultation signatures appear as very brief dips. Depending on the target stars, the occultation waveform may exhibit Fresnel diffraction effects. The star's size and the geometry of the occultation must be carefully taken into account to interpret the occultation data in terms of Kuiper belt object (KBO) size and distance. The observation programs dedicated to this type of research are described in this chapter. Three such programs have recently announced positive detections. These first results are described briefly, along with the information the data may provide. Potential results expected from these campaigns could help answer many questions concerning the Kuiper belt, its nature, and its relation with the Oort cloud: Is there an extended "cold" Kuiper belt? What is the size distribution for the Kuiper disk population? Is the maximum size of the KBO population decreasing with distance? What is the radial extent of the Kuiper belt? Is there a connection with the Oort cloud? What is the mass of the Kuiper belt? What fraction of KBOs are binaries? Are the smaller KBOs regular or elongated? These programs should also provide valuable data for theorists attempting to model solar system formation.

1. INTRODUCTION

For centuries, occultations of stars by the Moon have been used successfully for studying the binarity and angular size of stars. Nowadays, the stellar occultation method is commonly used to study the "dark matter" in the solar system, i.e., small objects or material invisible by direct imaging. The method consists of recording the flux of a star. Short-duration dips in the stellar flux indicate the passage of an object in front of the star.

A distinction must be made between occultations by known objects, for which we can predict the occultation conditions (timing, geometry, etc.), and occultations by unknown objects. The latter are random events. This chapter focuses on the serendipitous stellar occultation method, i.e., the search for random occultations by unknown/small objects belonging to the Kuiper belt.

The study of predictable occultation events has been applied to observe various solar system bodies. Such observations have been conducted using both large telescopes and smaller mobile instrumentation. The complementary nature of large and smaller instruments has proved crucial in producing the results obtained so far.

Stellar occultations have the potential to provide precise measurement of *asteroid* sizes and shapes. The applicability of this technique to the asteroids was understood as early as 1952 (*Taylor,* 1952). However, because of poor organization and equipment, as well as inaccurate predictions, the first successful occultation of a star by the asteroid Pallas was not observed until 1978 (*Wasserman et al.,* 1979). This observation permitted the determination of the dimensions of Pallas with an uncertainty of less than 2%, a precision never before achieved. The size determination, in turn, led us to derive the asteroid's density. To date, stellar occultation has proved to be the most accurate method (except for *in situ* exploration) for determining asteroid sizes and shapes, with the measurements of tens of asteroids as well as other bodies such as planetary satellites.

Stellar occultations can also be used to probe *planetary atmospheres*. This technique has proved to be a powerful tool for the detection of very tenuous atmospheres at microbar levels. Pluto's tenuous atmosphere was first detected by this means in 1985 (*Brosch,* 1995). The principle of the technique is to study the dimming of the starlight as it passes through the planet's atmosphere. The starlight interacts with the atmosphere through refraction and extinction.

Consequently, the stellar occultation method can provide the temperature, pressure, and density profiles of a planetary atmosphere with a typical vertical resolution of a few kilometers. Furthermore, depending on the quality and completeness of the dataset, this technique has sometimes been applied to determine local density variations, atmospheric composition, the presence of aerosol content, zonal wind speed, and temporal and spatial variations of the whole atmosphere. For example, the Pluto occultation of 2002 showed that Pluto's atmospheric pressure had, very surprisingly, increased by a factor of 2 since 1988, a phenomenon probably caused by frost-migration effects on the surface (see chapter by Stern and Trafton). Stellar-occultation studies of planetary atmospheres have included all solar system planets and many satellites like Triton, Titan, and Charon (see the review by *Elliot and Olkin,* 1996).

Finally, stellar occultations can also detect invisible material like *planetary rings and arcs* (see, e.g., *Sicardy et al.,* 1991). Thus, stellar occultations have led to the discovery of planetary rings and arcs around Uranus (1977) and Neptune (1984).

Stellar occultations by known members of the *Kuiper belt* are a new challenge, since they generally involve the use of fainter stars, and above all, bodies that subtend very small angles. Typically, a Kuiper belt object (KBO) subtends less than 30 milliarcsec on the sky. This makes occultations difficult to predict (*Denissenko,* 2004). The limitation on astrometric predictions of the shadow path on Earth severely complicates the logistics of the observations. Occultations by the largest KBOs have yet to be observed. The potential reward to be gained from detecting an occultation by a KBO is tremendous, however (*Elliot and Kern,* 2003).

First, this is a unique way to measure sizes at *kilometric* accuracy, using a number of observing stations on the ground and careful timing of the event. To measure the size, one does not need high photometric precision, hence small telescopes can be used. The size can be used, in turn, to derive the albedos of these bodies, and for those KBOs with satellites, their density.

Second, for the largest of these bodies, the sizes of which lie between the radii of Charon and Pluto, this is the only way to detect a possible tenuous atmosphere, down to a surface pressure of *30 nbar* for typical nitrogen, methane, or carbon monoxide atmospheres (see chapter by Stern and Trafton).

2. THE METHOD OF SERENDIPITOUS OCCULTATIONS

Stellar occultation is a powerful tool for detecting otherwise invisible objects in the outer solar system, using the method of serendipitous stellar occultation (*Bailey,* 1976). Using this method, one searches for random occultations of the background stars by passing objects. This permits us to study the invisible part of the KBO size distribution, for which the object's radius is less than a few kilometers, as well as the outer regions of the Kuiper belt. This method could also be used to obtain information about the larger members of the Oort cloud population.

2.1. Justification

The large distance from Earth to the Kuiper belt and the small size of KBOs limits the possibility of direct detection to the biggest objects. Current estimates suggest that there are a total of 10^5 KBOs larger than 100 km. The multikilometer radius objects have a differential size distribution $N(r) = N_0\, r^{-q}$, r being the object radius, with q = 4, after *Luu and Jewitt* (2002; see chapter by Petit et al.). One expects a shallower size distribution for smaller objects (*Bernstein et al.,* 2004). The position of the expected turnover radius is a critical clue to understanding the first stages of planetary formation in the outer solar system. As a hectometer-sized KBO at 40 AU is expected to have a magnitude of ≈40, reliable statistics on such small objects are unlikely to be obtainable by direct observation. Thus, exploration of the Kuiper belt by stellar occultations is the only way to obtain information about this population. Moreover, stellar occultation is less limited by the distance of the occultor, hence this technique can be used to explore the outer frontier of the Kuiper belt at ~10^2–10^5 AU, inaccessible by direct detection (Fig. 1).

A simple estimate of the power of the method can be made using geometrical optics: An object of radius r, passing in front of a star of angular radius α, creates a signal

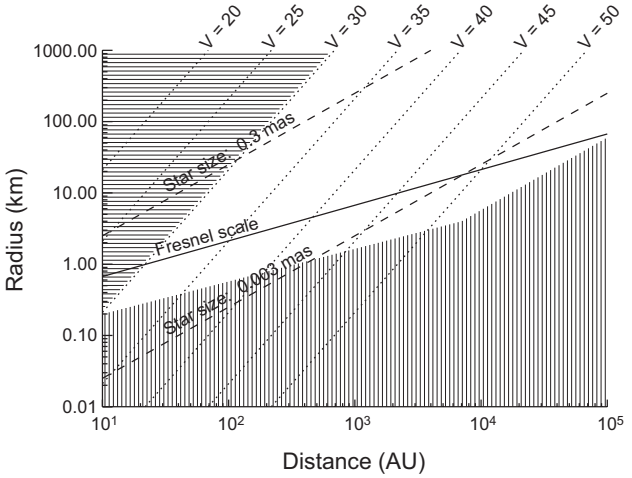

Fig. 1. Comparison of the direct detection method with the occultation method: The dotted lines show the visual magnitude. The dashed lines correspond to the projected stellar radius; the upper one corresponds to an M5 star with V = 12 and the lower one to an O5 star with V = 12. Occultations of stars larger than the Fresnel scale are geometric and the limit of detection is a fraction of the stellar radius. When the star is smaller than the Fresnel scale, the occultation is a diffracting phenomenon and the limit of detection is a fraction of the Fresnel scale. Objects in the white zone are invisible (V > 30) and can only be detected by occultation.

decay $\delta F = [r/(\alpha D)]^2$, where D is the object-to-Earth distance (for an impact parameter smaller than $\alpha D - r$). $\alpha D = R_*$ is the radius of the star projected at the distance of the occulting object. Note that if the star's apparent size is known, the occultation profile provides some information on the object's size without any hypothesis about its albedo. The angular sizes of the stars depend on their spectral and luminosity class and on their distance (see section 2.5). Figure 1 shows that, for a large proportion of stars, there would be full extinction for KBOs under 1 km in radius if the occultation were purely geometrical in nature. In reality, diffraction plays an important role for such occultations. And as a result, the occultations do not achieve full extinction. The diffraction shadow has specific properties that allow us to validate the detection of such events and also provide information about the size and distance of the occulting objects (see below).

The limitation of the serendipitous occultations method is that the objects detected are otherwise unknown, insofar as it is not possible to see them due to their very faint magnitude. Also, the detection of an object by occultation is not a reproducible observation. It is not a "discovery" because it is not possible to deduce a precise trajectory from a single observation, and hence observe it again later. Information about the physical properties of the Kuiper belt must be derived from statistical analysis of many occultation profiles or by the analysis of the very specific signature of single occultation profiles containing diffraction fringes. In addition, it is possible under some observing conditions to misinterpret occultation events caused by asteroids at much closer distances. Estimating the distance to the occultor by analysis of the diffraction fringes then becomes an important issue.

2.2. A Diffracting Phenomenon

Figure 1 shows that occultation of most stars is a simple geometric phenomenon. However, for some well-chosen stars (small angular size), occultations are a diffracting phenomenon up to a distance of 10^4 AU, i.e., for the outer Kuiper belt and the inner part of the Oort cloud.

Let us now focus on the properties of occultations involving diffraction. The light emitted by a point source (assumed to be at infinity so as to yield planar waves), incident on a sharp-edged obstacle (such as a KBO), is diffracted. Because of the Huygens-Fresnel principle of wave propagation, each point on a wave front may be considered as the center of a secondary disturbance giving rise to spherical wavelets, which mutually interfere. If part of the original wave front is blocked by an obstacle, the system of secondary waves is incomplete, so that diffraction fringes are generated. When observed at a finite distance D from the obstacle, this effect is known as "Fresnel diffraction," and falls within the scope of the Kirchhoff diffraction theory, which remains valid as long as the dimensions of the diffracting obstacles are large compared to the observed wave length λ and small compared to D (cf. *Born and Wolf,* 1980). The characteristic scale of the Fresnel diffraction effect (i.e., roughly speaking, the broadening of the object shadow) is the so-called Fresnel scale $F_s = \sqrt{(\lambda D/2)}$ (*Warner,* 1988). [Note that some authors give different definitions for the Fresnel scale: $\sqrt{(\lambda D/2\pi)}$, $\sqrt{(\lambda D)}$, or $\sqrt{(\lambda D)/2}$.] The Fresnel scale at 40 AU, for a wavelength of 0.4 μm (blue light), is 1.1 km and therefore diffraction must be taken into account when analyzing occultations by (under) kilometer-sized KBOs. Similarly, the Fresnel scale at 40 AU is 42 m for X-rays (0.6 nm). In fact, the Fresnel scale is a scaling factor of the profile. The shadows of occulting objects on Earth, *expressed in Fresnel scale,* are the same if the objects have the same size, *expressed in Fresnel scale.* This degeneracy can be broken if we have a measure of the relative KBO velocity in the sky plane and have a good knowledge of the star's apparent size. And finally, for non-monochromatic observations, the Fresnel scale must be averaged over the detector bandwidth and weighted by the detector response as a function of wavelength.

2.3. The Occultation Signature

The computation of the profile of a KBO occultation requires several steps, described below.

2.3.1. Computation of the diffraction pattern with a monochromatic point source. The modeling of the occultation of a point source by a disk is relatively easy and makes for a good approximation, even though most of the small KBOs are probably not spherical. Let us now consider the case of a monochromatic point source occulted by an opaque spherical object of radius ρ. If ρ denotes the distance between the line of sight (the star's direction) and the center of the object, and if the lengths r and ρ are expressed in Fresnel scale units, the normalized light intensity $I_r(\rho)$ is given by the following (see appendix B of *Roques et al.,* 1987):

Outside the geometric shadow ($\rho > r$)

$$I_r(\rho) = 1 + U_1^2(r,\rho) + U_2^2(r,\rho) - 2U_1(r,\rho)\sin\frac{\pi}{2}(r^2 + \rho^2) + 2U_2(r,\rho)\cos\frac{\pi}{2}(r^2 + \rho^2) \quad (1)$$

Inside the geometric shadow ($\rho < r$)

$$I_r(\rho) = U_0^2(\rho,r) + U_1^2(\rho,r) \quad (2)$$

where U_0,U_1, and U_2 are the Lommel functions defined by (for $x < y$)

$$U_n(x,y) = \sum_{k=0}^{\infty} -1^k (x/y)^{n+2k} J_{n+2k}(\pi xy) \quad (3)$$

where J_n is the Bessel function of order n.

Figure 2 shows the diffraction pattern of a circular object occulting a point star. It shows that objects a fraction

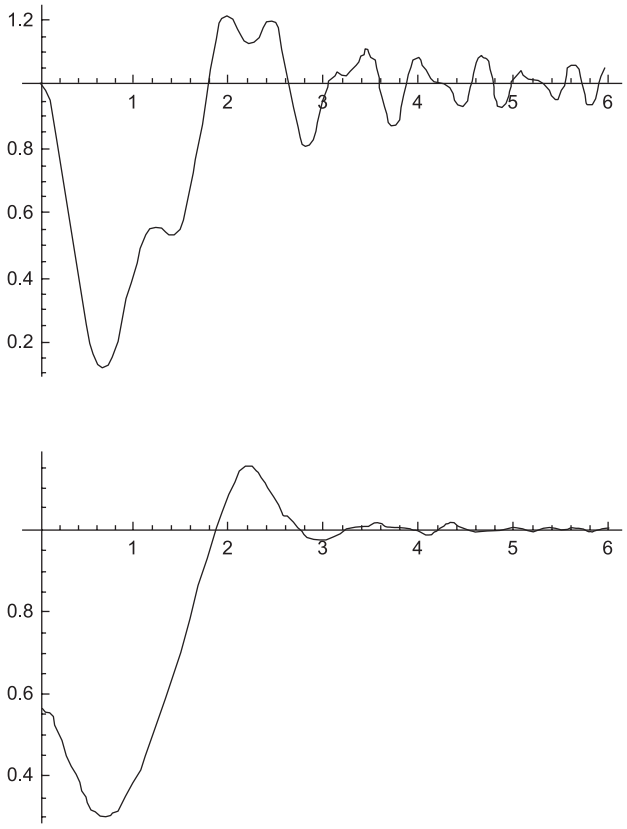

Fig. 2. Synthetic profiles for a 1-F_s radius occultor. The x axis unit is in Fresnel scale units. The upper diagram is for a projected stellar radius of 0.01 F_s, and the lower one for 0.5 F_s.

of a Fresnel scale in size produce a significant decrease in starlight. Furthermore, the size of the shadow is larger than the geometric shadow and overall, the diffraction fringes are visible at a large distance from the object. The computation of the diffraction pattern of an elliptical, or an irregular object is more complex (*Roques et al.,* 1987; *Roques and Moncuquet,* 2000). However, the diffraction fringes are significant for objects the size of which is on the order of, or smaller than, the Fresnel scale.

2.3.2. Wavelength dependency of the profile. As the profile depends on wavelength, averaging over the bandwidth of the detector smoothes the diffraction fringes. If the observation is done simultaneously at more than one wavelength (say, red and blue), the profiles of an occultation event are different in the different channels. The profile is larger, but shallower for red light. In fact, if expressed in Fresnel scales, the same object is smaller in the red than in the blue. This property can be used to verify the authenticity of the event.

2.3.3. Convolution of the profile with the projected disk of the target star. If we consider the light source to be a distributed rather than a point source, we must convolve the occultation profile with the source shape. In the case of a star, the source shape is really a disk. To perform the convolution, one needs to know the star's angular size with good precision. The normalized light intensity measured during the occultation of a stellar disk of apparent radius R_* (expressed in Fresnel scale) is

$$I_r^*(\rho) = \frac{2}{\pi R_*^2} \int_0^{R_*} s\, ds \int_0^{\pi} I_r\left(\sqrt{\rho^2 + s^2 + 2\rho s \cos\theta}\right) d\theta \quad (4)$$

The diffraction fringes are strongly smoothed when the star's apparent size is larger than roughly half the Fresnel scale (Fig. 2). When the star's apparent size is larger than the Fresnel scale, the occultation shadow is closely approximated by the geometric occultation case, and the decrease of light intensity is simply the ratio of the surface area of the occultor to the surface area of the star disk as projected at the occultor's distance.

2.3.4. Dependency on integration time. The profile must also be averaged over the integration time (i.e., the time taken for one data sample). The occultation dips are very brief events, so the sampling rate must be fast enough to provide good resolution of the occultation profile (see below).

2.4. The Geometry of the Observation

If the KBO has a circular orbit in the ecliptic plane around the Sun, its velocity v in the sky plane is given by

$$v = v_E\left(\cos\omega - \sqrt{\frac{1}{D_{AU}}}\right) \quad (5)$$

where D_{AU} is the heliocentric distance of the KBOs in AU, v_E is the Earth's orbital speed ≈30 km/s, and ω is the angle between the KBO and the antisolar direction (called "opposition" hereinafter). ω is called the observation angle (Fig. 3).

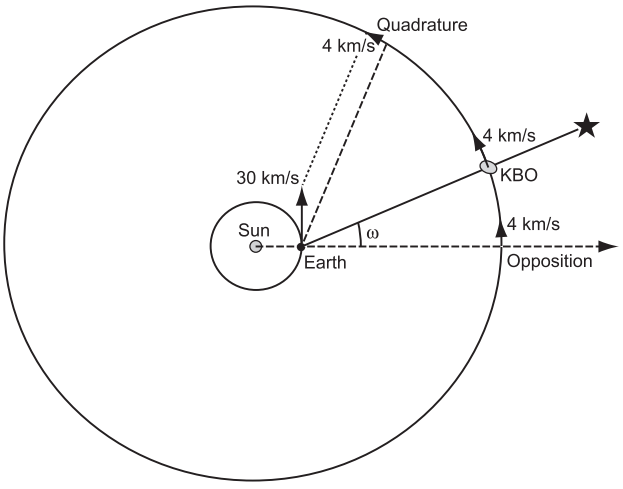

Fig. 3. Geometry of an occultation by a KBO, showing the observation angle ω.

Because v depends on the distance of the occulting objects, so do both the duration of the occultation ($dt \alpha 1/v$) and the number of occultations ($N_{occ} \alpha v$). The velocity is maximum toward the opposition and minimum toward a direction, called the "quadrature" hereinafter, for which $\cos \omega = 1\sqrt{D_{AU}}$. This property allows us to discriminate between occultations by a KBO population and an asteroid population, because quadrature for KBOs and asteroids are at different positions (see Table 4 in *Roques and Moncuquet,* 2000).

At 40 AU, we get $v \approx 30(\cos w - 0.16)$ km/s $\approx(\cos w - 0.16)$ mas/s, the velocity is ≈25 km/s toward the opposition and the quadrature at ≈81°. An occultation by a small KBO could last from about 0.1 s to a few seconds, as ω goes from the opposition to the quadrature. If the data acquisition rate is not fast enough, the occultation profile is degraded. For good resolution of the events, the acquisition rate must be larger than v/F_s. To satisfactorily resolve events toward opposition, this rate must be greater than 600 Hz at 0.6 nm and 20 Hz at 0.4 μm.

When the acquisition rate is not fast enough, observations toward quadrature may still detect bodies that are invisible toward opposition (because their occultation dips are too brief to be detected). Observing toward quadrature makes this technique less restrictive in terms of the acquisition rate. Thus, *Brown and Webster* (1997) proposed to search for KBO occultations toward quadrature with the MACHO experiment.

2.5. The Target Stars

Selecting appropriate target stars is critical to the success of any occultation observation program. The smaller the occulted star, the smaller the detectable KBO, and because small KBOs are more numerous, the higher the occultation rate. It is essential that the selected target stars project a disk onto the Kuiper belt plane that is of the same size or preferably smaller than the Fresnel scale.

The radius of the star, projected at the distance D, is $R_* = \alpha D$, so that

$$\log R_* = -\frac{V}{5} = \frac{M}{5} + \log\left(\frac{R}{R_S}\right) + \log\left(\frac{DR_S}{d_{pc}}\right) \qquad (6)$$

where V is the apparent magnitude of the star, M its absolute magnitude, and R its radius; R_S is the radius of the Sun, and $d_{pc} = 10$ pc. One way to favor a small projected stellar radius is to reduce the apparent magnitude. Unfortunately, this degrades the signal-to-noise ratio of the lightcurve. Another method is to consider hot stars, which, for a given apparent magnitude, project a smaller angular size. An O5 star of V = 12 has a projected radius of 130 m at 40 AU. With the same magnitude, an M5 star has a projected radius of 10 km (Fig. 1). The above equation does not take into account interstellar extinction or reddening. If extinction is significant, the apparent magnitude will be underestimated and so will the star's apparent size. However, if the reddening is not taken into account, the star is hotter than estimated, and the apparent size is smaller than estimated. An estimate for interstellar extinction and reddening can be derived from studies such as that done by *Kharchenko et al.* (1996) toward the center of the galaxy. However, the errors associated with any such estimates are likely to be large. The stellar size distribution is considered by *Cooray* (2003) in a geometric framework.

The magnitude and spectral class of the target stars need to be carefully chosen. The effective telescope aperture sets the lower limit criterion for a target star's observed magnitude. Below this limit, scintillation noise and photon noise degrade the photometry to the point where it is no longer usable for occultation work. Unfortunately, the above selection criteria dictate that for any given range of magnitudes, the vast majority of stars are unsuitable as occultation target candidates. The hottest stars have the highest light output per unit of surface area. It so happens that the very hottest stars (types O, B, and A) provide the best candidates for occultation work. As an example, for a 1.2-m telescope fitted with a high-efficiency detector and no filter, the limiting magnitude for KBO detection work is V ~ 12. Stars of type O, B, and A with $10 < V < 11.5$ are suitable for detecting KBOs down to a radius of ~250 m when observing at opposition. Field crowding can be a problem, particularly toward the center of the galaxy. Long exposure plates in the vicinity of each star need to be checked to make certain that confusion is not a problem.

Finally, the distribution of KBOs dictates that all observations be carried out on target stars located close to the ecliptic. The galactic plane crosses the ecliptic at two locations on the sky. The large number of stars at these two locations makes finding suitable target star candidates easier for any observation program. Furthermore, one crossing occurs very close to the direction of the galactic center. This particular location provides the densest possible star fields anywhere on the sky. However, in the long term, exploring the Kuiper belt by the occultation method will make it necessary to find appropriate fields all along the ecliptic.

3. TELESCOPES AND INSTRUMENTATION

Choosing a telescope and high-speed instrumentation for KBO occultation work involves a judicious selection of various conflicting parameters, all of which affect the probability of detecting occultation events. This section describes instruments used in the various programs dedicated to the detection of KBOs by occultation. It does not cover the X-ray satellite used for this subject (see below).

3.1. Telescope

Using a wide-field telescope and appropriate detection instrumentation, it is possible to monitor many suitable target stars in the same field of view. This greatly increases the probability of detecting occultation events. However, the

signal-to-noise ratio will be relatively poor due to the effects of scintillation — typically a 5% noise level for a 1-m-aperture telescope (see *Young,* 1967; *Warner,* 1988). If one employs a larger telescope (e.g., 4-m-aperture or larger), the field of view will be much smaller. However, due to the larger telescope aperture, it will be possible to monitor fainter stars. With a suitable detector, a 1% noise level can be achieved, and this should be sufficient to permit diffraction fringes to be observed.

The issue of whether to attempt observing diffraction events needs to be assessed in terms of system requirements. Any system targeting diffraction-based occultation events must be capable of high photometric precision (ideally ~1% or better), and must use a narrowband blue filter and target stars whose projected disk size is preferably less than one-tenth that of the Fresnel scale. These criteria imply that one must use the largest possible telescope, along with a detector capable of fast, high-precision photometry. This latter constraint usually implies the use of ultra-rapid camera, which immediately limits the number of target stars that can be observed simultaneously to a few at most. Thus the probability of detecting any event will be low, thereby necessitating many hours of monitoring.

If one uses a wide-field telescope to monitor 100 or more suitable target stars simultaneously, the chances of detection are greatly improved, albeit under somewhat noisy photometric conditions. To obtain the best possible photometry, such observations should be carried out using a high-efficiency detector without any intervening filter. The demands on medium-sized telescopes are not as great, so longer observing runs are feasible.

3.2. Detectors Suitable for Multi-Object Occultation Work

Two types of detector suitable for multi-object occultation work are available. A multi-photometer instrument can simultaneously record the flux from several stars with a high sampling rate and good signal-to-noise ratio (*Roques et al.,* 2003). Another approach consists of using a CCD camera to image the target star field directly. Unfortunately, the readout time for large CCD images is too slow for satisfactory KBO occultation work. To compound the problem, CCDs tend to be noisy when working in fast readout mode. By judicious selection of target field, CCD camera type and special programming techniques — such as pixel binning and window readout — it is possible to acquire data at a sufficiently high rate (e.g., 50 ms integration time) and with a satisfactory signal-to-noise ratio to have a chance of detecting KBO occultations. An observation of a typical KBO occultation using the above-mentioned approach is likely to yield two to three data point detections. A fiber-based multi-object spectrograph/CCD camera, combined with a suitable setup and CCD control software, allows acquisition rates as fast as 10 ms. Using such a scheme, a typical occultation event consists of 10 to 15 data points. Thus, each event can be nicely resolved. As an additional bonus, some information about the shape of the occulting object can be gleaned from the occultation waveform. Finally, new CCD technology now permits the use of very fast response cameras with a 20-ms integration time (*Dhillon and Marsh,* 2001) (see also *www.shef.ac.uk/physics/people/vdhillon/ultracam/*).

4. DATA REDUCTION

Detection of occultations relies on monitoring the light received from one or more stars. The acquired data will vary in format, noise content, and event characteristics, depending on the nature of the instruments used for the acquisition. For CCD camera images, the target stars represent signal peaks in two-dimensional signal space. To compute the lightcurves, one needs to choose an aperture size. The choice is done in a manner that minimizes the r.m.s. fluctuations of the lightcurve. For CCD images derived from a multi-object spectrograph, the light is collected from each target star in a separate fiber. The fibers are then physically aligned along a row in front of the CCD camera. This permits fast acquisition, as only the first few rows of the CCD image need to be read.

The aim of data reduction is to find signal changes similar to those expected for a distant KBO passing in front of a target star. Event-detection algorithms may be based on simple level change detection, σ threshold detection, or cross-correlation with one or more suitable event mask(s). This latter technique is a powerful means of detecting all types of events, including Fresnel diffraction waveforms, in the presence of noise. Such waveforms may be mathematically synthesized, and the parameters tuned for the relevant detection conditions.

The small KBOs we are seeking to detect by occultation are effectively invisible from Earth with all other present-day observing techniques. We can never be 100% certain that a dip in the lightcurve of a star is due to an occulting KBO. Observational artifacts can be due to instrumental effects, near-Earth phenomena and unknown effects. Simple tests can be performed to eliminate most of the following artifacts:

1. *Correlated events.* Systems that simultaneously monitor several nearby stars possess a powerful means of discriminating against false detections. An event that occurs simultaneously on more than one star (hereafter called a correlated event) *must* be an observational artifact! Kuiper belt objects are far too rare, small, and distant to occult more than one star at a time. As an example, a bird or a plane flying through the telescope field of view will cause a brief reduction in light intensity. This reduction is proportional to the percentage of the aperture that an object obstructs as it flies past. This reduction in intensity occurs for all objects in the field of view, not just for a single star. Thus, a correlated event is generated. Other examples of artifacts that can cause correlated events include clouds passing through the field of view, electronic glitches, and telescope tracking errors.

2. *Nearby telescopes*. Simultaneous observation using two nearby telescopes permits us to confirm the reality of an occultation by an interplanetary object. The distance between the telescopes must be smaller than one Fresnel scale unit. The simultaneity of an event serves to confirm the reality of the occultation. The observation with several telescopes on an east-west line, could, in principle, permit us to retrieve the event with a time shift, which, in turn, gives us information about the KBO shadow velocity.

3. *Multi-wavelength observations.* The profiles of an occultation event observed at different wavelengths are different: The dips are larger and shallower in red than in blue. This difference between the profiles will confirm that it is a diffracting event. The comparison between the two profiles gives information about the size and the distance of the occulting KBO.

4. *Single data point events.* In order to assist with differentiating against artifacts, an observation scheme must be capable of resolving KBO-related occultation events into more than just one data point. For example, single-data-point events may be caused by Earth-orbiting objects or cosmic rays. An artificial satellite will completely extinguish a star during a millisecond.

To check for instrument-related artifacts linked to detection electronics, it should be possible to run a check by observing a suitably illuminated white screen for an extended period of time during the day. Any artifacts generated by the instrumentation will be immediately evident.

5. *Profile fitting*. Occulation profiles have special signatures that depend on the observing conditions, the size of the target star's projected disk and the shape, and size of the occultor(s). For example, Fresnel diffraction simulations show that occultations by small KBOs have a characteristic shape and should never reach 100% depth. This is a powerful sanity check. Also, correlating observed events with synthetic profiles permits us to further probe the reality of the occultation.

6. *Event statistics.* To further differentiate between real events and artifacts, one can make use of event statistics. The event statistics should change with the angle of observation ω (see section 2.4). On the one hand, the event rate should drop as ω decreases. For example, toward $\omega = 60°$, the event rate for any KBO size should drop by a little over one-half with respect to the events rate at $\omega = 30°$ (equation (5)). However, as we observe closer toward quadrature, the observing geometry permits us to detect progressively smaller objects due to the longer event duration. As smaller objects are thought to be more numerous, this effect may partially counteract the reduction due to the decreasing probability of detection.

Similarly, there are other statistics-based checks that can be performed for the purpose of event verification, e.g., the comparison of dips with stars of different sizes, such as O/A stars and K/M stars with the same visual magnitude: In the latter, the stellar disks projected onto the Kuiper belt plane will be too large to produce any deep occultation events.

Another very robust test is the monitoring of stars well away from the ecliptic. Here, we should detect very few events, because we are no longer looking through the main part of the Kuiper belt.

5. ANALYSIS OF THE OCCULTATION EVENTS

5.1. Population Parameters

Occultation data provides an instantaneous view of the position of the KBOs in the sky plane, but does not give access to the orbit parameters. This is because it is not possible to derive the orbit parameters of any object from a single observation. Note also that the density in the sky plane of KBOs detected by occultation cannot be compared to that of objects observed directly because the sensitivity of the two methods to the distance parameter is different. If the observations provide enough events in a given configuration (star size, position in the sky, value of the angle of observation ω), and taking into account the geometry of the observation, it may be possible to use the event rate to estimate the density of KBOs in the sky plane. Unfortunately, in occultation work, there exists a degeneracy between the size of a KBO, its distance, and the impact parameter of the occultation. This is because there are three unknowns and only two measured variables (the event duration and its depth). Under certain conditions, this degeneracy can be lifted. For example, a mean value for the distance to the Kuiper belt can be derived from observations done at two (or more) widely separated observing angles, ω.

If a fixed distance is assumed, the density in the sky plane gives an indication of the density of objects. This, in turn, can be compared with the large KBO size distribution. Fitting diffraction profiles with synthetic profiles gives access to the velocity of the occultor in the sky plane. This permits us to estimate the distance of the object, if we make some assumptions about the orbit (e.g., circular orbit). On the other hand, occultations will give a direct measure of the positions of the occultors with respect to the ecliptic plane, and this provides information about the thickness and the potential azimuthal variations of the density of the Kuiper belt. If the occultation profiles are well defined, comparison with synthetic profiles could give some information about the shape of the objects, and on their roundness. The proportion of binaries can also be constrained by occultation data.

5.2. Lower Limit of Detection

Noise in the measured lightcurve imposes a lower limit on the detectability of dips due to occultation events. The level of scintillation noise, in turn, is primarily governed by the telescope aperture (see section 3.1). The level of photon noise is governed by the star magnitude. On the other hand, the smallest detectable size also depends on whether diffraction fringes are present. If d_{min} is the limit in the detectable event depth, the radius of the detectable ob-

ject is roughly $\sqrt{d_{min}/3} \cdot F_s$ for diffracting occultations and $R_*\sqrt{d_{min}}$ for geometrical occultations. F_s is the Fresnel scale (section 2.2) and R_* is the stellar radius projected at the KBO distance (section 2.5). For a 1-m (4-m) telescope, these limits are ≈0.3 F_s (0.15 F_s) and ≈0.4 R_* (0.2 R_*). Figure 1 shows that if the projected stellar disks are smaller than the Fresnel scale, objects of few hundred meters in radius are detectable.

The integration time can also limit the shortest detectable events. If the acquisition frequency is smaller than v/F_s, the smaller objects may not be detected because the occultation duration is shorter than the integration time. Information about smaller objects can best be obtained at larger observation angles ω, since v decreases with increasing observing angle (see section 2.4).

6. THE RESEARCH PROGRAMS

Several research programs are in progress using different approaches. The expected number of detections with each program is very difficult to estimate because it varies with hypotheses on the size and spatial distribution of KBOs and on the efficiency of the method. Two programs have very recently announced positive detections: three detections for the Paris program (*Roques et al.,* 2006), and hundreds of events from the University of New South Wales (UNSW) program (*Georgevits,* 2006).

6.1. The Taiwan-America Occultation Survey Program

The Taiwan-America Occultation Survey (TAOS) project is the first project to conduct a survey of the Kuiper belt using stellar occultations (*Alcock et al.,* 2003). This collaboration, involving the Lawrence Livermore National Laboratory (USA), Academia Sinica and National Central University (both of Taiwan), and Yonsei University (South Korea), uses the occultation technique in conjunction with an array of four wide-field robotic telescopes. Their aim is to estimate the number of KBOs of size greater than a few kilometers radius. The 50-cm f/1.9-aperture telescopes simultaneously point to a 3 deg^2 area of the sky and record light from the same ~1000 stars (V < 14). The array is located in the Yu Shan (Jade Mountain) area of central Taiwan (longitude 120° 50' 28"; latitude 23° 30' N). The detection scheme is operating in real time, to be able to alert more powerful telescopes that could then follow the motion of a potential occultor. A large amount of data is generated on a nightly basis, yielding about 10,000 GB of data and 10^{10}–10^{12} occultation tests per year. The expected number of occultations ranges from a few to a few hundreds.

Each telescope is equipped with an SI800 2 K camera, and the data acquisition system runs on a shutterless mode. The chip integrates ("pause") and then reads out a block of pixels ("shift") once at a time, instead of the whole frame. This "pause-and- shift" operating mode permits it to sample stellar lightcurves at up to ~5 Hz.

Three telescopes have been operational since early 2005. Some 10^9 stellar photometric measurements have been collected. So far, no events have been detected. A few predicted asteroid occultations (e.g., 51 Nemausa and 1723 Klemola) were recorded to demonstrate the capability of the system.

6.2. The Paris Program

After a theoretical analysis of the serendipitous occultation method (*Roques and Moncuquet,* 2000), the team from Observatoire de Paris lead by F. Roques conducted several observation campaigns. Some of the results obtained so far are:

1. The first observations were carried out at Pic du Midi with the 2-m Bernard-Lyot Telescope with a multi-object photometer. These observations showed the relevance of this approach, brought a first constraint on the size distribution of KBOs, and delivered a possible profile of detection of KBOs (*Roques et al.,* 2003).

2. Observations have been conducted on larger telescopes: the La Palma 4.2-m William Hershel Telescope and the European Southern Observatory, Paranal, 8.2-m, Very Large Telescope with the ultrarapid CCD Ultracam camera. *Roques et al.* (2006) reported the first and unambiguous detection of hectometer-sized KBOs at a few hundred AU.

The approach of the Paris team is to monitor few well-chosen single stars toward opposition with the ultrarapid triple-beam CCD Ultracam (*Dhillon and Marsh,* 2001) (see also *www.shef.ac.uk/physics/people/vdhillon/ultracam/*). This instrument allows a very fast acquisition rate and observations at three different wavelengths. Observations are made in two windows, each 34 × 34 $arcsec^2$, with an acquisition frequency of 42 Hz. Two (or more) stars are observed simultaneously. Comparison of the lightcurves from the different stars eliminates "false events" due to observing mishaps (of technical or human origin) and arising from near-Earth artifacts (clouds, birds, satellite, etc). If an event is observed simultaneously or quasi-simultaneously on more than one star, it can be assumed to be an Earth-connected artifact.

The detection algorithm used by the Paris team computes the standard deviation of the stellar flux and filters out all fluctuations below a 5σ standard deviation level. High-frequency fluctuations, either due to cosmic rays, clouds, or electronic glitches, have a clear signature and are eliminated by visual examination of the time series.

A further, more robust statistical technique is used to isolate sources of noise such as scintillation. This technique is known as the vectorial "Variability Index" (VI). For a given interval, one can define VI(int) with coordinates equal to the standard deviations of the normalized stellar flux in two different wavelength bands. Each standard deviation is computed relatively to the mean standard deviation of the dataset and expressed in units of standard deviation: sig = stddev(int) is the standard deviation for the interval int; meansig is the mean standard deviation of the data (for the whole night), then VI(int) = (sig(int)–meansig)/stddev(sig).

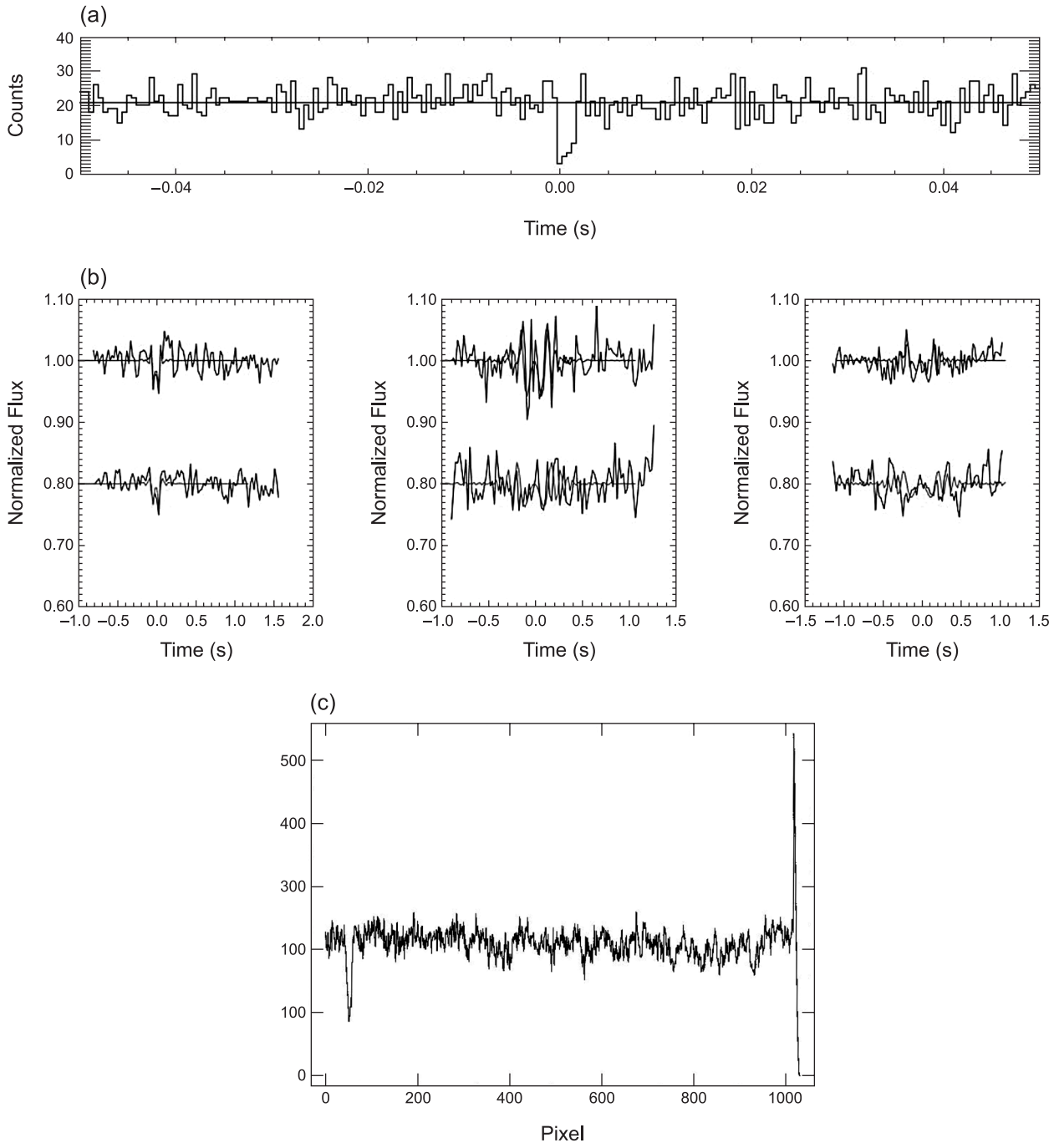

Fig. 4. Examples of events: **(a)** X-ray event (*Chang et al.,* 2006); **(b)** Paris team events (*Roques et al.,* 2006); **(c)** UNSW event. The 1000 pixels in the x-axis correspond to 10 seconds of acquisition.

For a purely random dataset, a two-dimensional plot of VI appears as an isotropic cloud of vectors centered on the origin. The distribution is Gaussian, therefore concentrated around the mean. Consequently, any deviant point should represent the detection of a nonrandom event.

The Paris team observations reported the detection of three objects (*Roques et al.,* 2006) using this technique. Cumulative observations from the William Hershel Telescope and from the Very Large Telescope yielded a first result on the density of objects on the sky plane. The number of occultors with a profile depth of ~5% (a 0.1-F_s object) is $2 \pm 1 \times 10^{10}$ deg^{-2}. The comparison of the dips with synthetic profiles suggests that one object is 100 m in radius and located at 10–20 AU and the two others are 300-m objects at 140 and 210 AU (Fig. 4). Other observations will be conducted to add to these results.

An additional program with the satellite Corot, a high-precision photometry mission, will be dedicated to the search

of occultation by KBOs. The main objectives of this satellite are stellar seismology and the search of exoplanetary transits. Such a program will provide information on the population of decameter-sized objects.

6.3. The University of New South Wales (UNSW)/ Anglo Australian Observatory (AA) Program

A pilot set of occultation observation runs were conducted on the UNSW 0.5-m Automated Patrol Telescope in 2004 by G. Georgevits' team. The target field was the O–B association cluster NGC6611, located at a distance of 2.2 Kpc. Using the CCD techniques outlined above, a 50-ms integration time was achieved. Some two-pixel events were detected. The results appeared sufficiently favorable to warrant further observational work using a larger telescope. To follow up on this work, the 1.2-m UK Schmidt Telescope (UKST)/6df multi-object spectrograph (6° field) was used to undertake a more ambitious occultation program. The UKST is a survey telescope with a very wide field of view. It was originally designed to photograph 6.6° × 6.6° areas of the sky. It is now been fitted with a fiber-based multi-object spectrograph.

A new "through" mode of operation was developed for the multi-object spectrograph to support the UNSW/AAO occultation program. This involved using the spectrograph without an intervening diffraction grating. In addition, the acquisition software was modified to permit a very fast 10-ms integration time. The CCD camera has peak efficiency of around 65%, and better than 40% efficiency over the range 400–800 nm. The UNSW/AAO Occultation Observation Program was conducted over a period of four months in 2005. Data was acquired at observation angles of 30° before opposition, and 30° and 60° past opposition. The spectrograph equipment configuration permitted simultaneous monitoring of ~90 specially selected target stars. A total of nearly 7000 h of stellar lightcurve data was acquired.

The target stars consisted mostly of O-, B-, and A-class stars. They were selected from 4° × 4° fields located close to the center of the galaxy, centered on the point where the ecliptic crosses the galactic equator. Target star magnitudes ranged from V = 10.5 to 11.5, with most stars having B–V < 0. It is difficult to get an accurate value for reddening or extinction when observing toward the center of the galaxy, due to the copious amounts of gas and dust in this region. "Best estimate" based on *Kharchenko et al.* (1996) allows us to say that most target stars used for this work have a disk radius in the range 300–600 m when projected at 40 AU.

Most of the artifact identification/elimination techniques and statistical checks described above have been employed as part of the data verification process. At this stage, it appears that a large number of occultation events have been detected (*Georgevits,* 2006). An example is given Fig. 4. The analysis of the data is still in progress and the implications relating to the KBO population have yet to be derived.

6.4. The Canadian Project

Another project is led by JJ Kavelaars of the Queen University of Kingston, Canada. Their approach consists of correlating the observed photometric time series with synthetic diffraction patterns. They have analyzed 6.5 star-hours of 40-Hz photometry to search for occultations but found no viable candidate event. The search algorithm uses the cross-correlation of template occultation events with a time series. Several different templates are used to cover the parameter space of KBO size and distance, and each one is also run at 20 different impact-parameter distances. The detection algorithm flags any point in the time series that produces a peak in the cross-correlation greater than six times the standard deviation of the cross-correlation series. Then the candidate events are subsequently evaluated by eye.

Artificial occultation events were added to the data before the detection process was run to determine the efficiency of the algorithm. With their data, they were able to recover the artificial events corresponding to objects as small as 250 m in radius, and having impact-parameters up to 1 km. This implies a cumulative surface density less than 2.7×10^{10} deg^{-2}.

They also developed a way to simulate scintillation noise and produce artificial time series. By running their detection algorithm on these artificial data, they were able to find candidate events with fairly high significance (6.4 times the standard deviation of the cross-correlation series was the highest). Unfortunately, this means that the noise can mimic occultation events quite convincingly. What remains to be done is to determine the rates at which false-positive events will occur due to scintillation noise. To do this, they are running their detection code on artificial time series made at different noise levels, and with different slopes in the power spectrum.

6.5. Proposed Space-Based Project

Whipple is a space-based occultation survey of the outer solar system proposed by the Smithonian Astrophysical Observatory, Ball Aerospace, and the Jet Propulsion Laboratory. The aim of this mission is to measure the size distribution of KBOs down to 300 m, to map out the spatial distribution of the Kuiper belt, to determine if a Sedna-like population exists, and to determine the KBO population and distribution in the inner and outer Oort cloud. The proposed spacecraft is based on a 95-cm Schmidt optical system with a 100-deg^2 field and a hybrid CMOS focal plane array (Rockwelle HyViSI/Hawaii-2RG). The flux of 140,000 stars will be recorded at a frequency of 40 Hz. Whipple will go into an Earth-trailing orbit and will scan fields at all ecliptic longitudes and latitude. The raw data rate of 1 Gbps requires significant onboard processing. The expected event rate is thousands to tens of thousands per year for KBOs. Several tens of Oort cloud objects could also be detected per year. *Nihei et al.* (2007) describes this project and com-

pares it with the TAOS observations and observations with a 6.5-m telescope.

6.6. X-Ray Occultation Data

X-ray occultations may stand a good chance of revealing the existence of small KBOs as long as the background X-ray source is bright enough to allow statistically meaningful determination at short timescales. Scorpius X-1 is the brightest and first-discovered X-ray source outside the solar system. Moreover, it is only 6° north of the ecliptic. Analysis of archival data sets of this object by the satellite RXTE has been conducted by the Taiwanese team of H. Chang. The Proportional Counter Array (PCA) instrument (2–60 keV) onboard RXTE has registered a raw count rate of about 10^5 counts per second. This count rate enables them to perform an examination of the lightcurve at timescales as short as 1 ms to search for possible occultations. The first results (*Chang et al.,* 2006) show events compatible with occultation by KBOs of a few tens of meters (Fig. 4). Unfortunately, these reported dip events seem to be contaminated by those due to high-energy particles (*Jones et al.,* 2006). A definite identification of X-ray occultation events probably cannot be achieved until adequately configured observations are conducted in the future (*Chang et al.,* 2007).

7. CONCLUSIONS

The exploration of the Kuiper belt using the method of serendipitous stellar occultations has been under development for several years. The very first results appeared in 2006. The occultation method permits us to detect subkilometer-radius objects throughout the solar system and in particular in the region of the giant planets and beyond. This method also provides a potential way of detecting cometary nuclei in the Oort cloud. The main limitation of the occultation technique is that most of the detected objects cannot be observed again. Hence, information about the Kuiper belt population can only come from statistical analysis.

The method does not allow determining the distance of the occulting object from the analysis of a single profile. An indirect method is to map the spatial distribution of several events, because this spatial and temporal distribution depends on the distance of the KBO population. This difficulty could be bypassed by using very small angular size target stars. The diffraction profiles would then provide information on the distance and size of the occulting object. The size distribution of the population can be retrieved if the distance to the occultors is known. Three different research programs based on this technique have recently announced positive detections. These promising results show that there exists a large population of small objects in the outer solar system and that the occultation method is a powerful tool to explore this population. The analysis of these results is likely to bring very significant progress in a short time frame. The Paris program announced the possible existence of an extended cold disk. More detections and comparisons with other programs will further test these results and bring answers to decisive questions regarding the size and spatial distribution of the Kuiper belt, its connection with the Oort cloud, the shape distribution of KBOs, and the percentage of binary objects in the population.

A connected research field, not treated in this chapter, is occultations by the known KBOs. It will soon give important results about the size, shape, and density of the largest KBOs. Indeed, only the largest KBOs allow sufficiently precise astrometric predictions. This improved knowledge of the structure of the Kuiper belt, and in particular of the unperturbed part of the disk, will provide an important input for a more complete model of solar system formation.

Acknowledgments. It is a pleasure to thank J. Elliot, an anonymous referee, R. Courtin, and the editor for very useful comments that greatly improved this chapter.

REFERENCES

Alcock C., Dave R., Giammarco J., Goldader J., Mehner M., et al. (2003) TAOS: The Taiwanese-American Occultation Survey. *Earth Moon Planets, 92,* 459–464.

Bailey M. E. (1976) Can invisible bodies be observed in the solar system. *Nature, 259,* 290–291.

Bernstein G. M., Trilling D. E., Allen R. L., Brown M. E., Holman M., et al. (2004) The size distribution of trans-neptunian bodies. *Astron. J., 128,* 1364–1390.

Born M. and Wolf E. (1980) Elements of the theory of diffraction. In *Principles of Optics, Sixth Edition*, pp. 370–458. Pergamon, New York.

Brosch N. (1995) The 1985 stellar occultation by Pluto. *Mon. Not. R. Astron. Soc., 276,* 571–578.

Brown M. J. I. and Webster R. L. (1997) Occultations by Kuiper belt objects. *Mon. Not. R. Astron. Soc., 289,* 783–786.

Chang H., King S., Liang J., Wu P., Lin L., et al. (2006) Occultation of X-rays from Scorpius X-1 by small trans-neptunian objects. *Nature, 442,* 660–663.

Chang H.-K., Liang J.-S., Liu C.-Y., and King S.-K. (2007) Millisecond dips in the RXTE/PCA light curve of Sco X-1 and trans-Neptunian object occultation. *Mon. Not. R. Astron. Soc., 378,* 1287–1297.

Cooray A. (2003) Occultation searches for Kuiper belt objects. *Astrophys. J. Lett., 587,* L125–L128.

Denissenko D. V. (2004) Occultations of stars brighter than 15 mag by the largest trans-neptunian objects in 2004–2014. *Astron. Lett., 30,* 630–633.

Dhillon V. S. and Marsh T. (2001) ULTRACAM studying astrophysics on the fastest timescales. *New Astron. Rev., 45,* 91–95.

Elliot J. L. and Kern S. D. (2003) Pluto's atmosphere and a targeted-occultation search for other bound 2b6 atmospheres. *Earth Moon Planets, 92,* 375–393.

Elliot J. L. and Olkin C. B. (1996) Probing planetary atmospheres with stellar occultations. *Annu. Rev. Earth. Planet. Sci., 24,* 89–123.

Georgevits G. (2006) Detection of small Kuiper belt objects by stellar occultation. *Bull. Am. Astron. Soc., 38,* 551.

Jones T. A., Levine A. M., Morgan E. H., and Rappaport S. (2006)

Millisecond dips in Sco X-1 are likely the result of high-energy particle events. *The Astronomer's Telegram, 949.*

Kharchenko et Schilbach E. (1996) Schmidt plate toward the galactic centre. 2. Stellar statistic in the direction of the Sagittarius-Carina arm. *Astron. Nachr., 317(2),* 117–126.

Luu J. X. and Jewitt D. C. (2002) Kuiper belt objects: Relics from the accretion disk of the sun. *Annu. Rev. Astron. Astrophys., 40,* 63–101.

Nihei T. C., Lehner M. J., Bianco F. B., King S.-K., Giammarco J. M., and Alcock C. (2007) Detectability of occultations of stars by objects in the Kuiper belt and Oort cloud. *Astron. J., 134,* 1596–1612.

Roques F. and Moncuquet M. (2000) A detection method for small Kuiper belt objects: The search for stellar occultations. *Icarus, 147,* 530–544.

Roques F., Moncuquet M., and Sicardy B. (1987) Stellar occultations by small bodies: Diffraction effects. *Astron. J., 93,* 1549–1558.

Roques F., Moncuquet M., Lavilloniere N., Auvergne M., Chevreton M., et al. (2003) A search for small Kuiper belt objects by stellar occultations. *Astron. J., 594,* L63–L66.

Roques F., Doressoundiram A., Dhillon V., Marsh T., Bickerton S., et al. (2006) Exploration of the Kuiper belt by high precision photometric stellar occultations: First results. *Astron. J., 132,* 819–822.

Sicardy B., Roques F., and Brahic A. (1991) Neptune's rings, 1983–1989 ground-based stellar occultation observations. *Icarus, 89,* 220–243.

Taylor G. E. (1952) An occultation by a minor planet. *Mon. Not. Astron Soc. South Africa, 11,* 33.

Warner B. (1988) *High Speed Astronomical Photometry.* Cambridge Univ., Cambridge.

Wasserman L. H., Millis R. L., Franz O. G., Bowell E., White N. M., et al. (1979). The diameter of Pallas from its occultation of SAO 85009. *Astron. J., 84,* 259–268.

Young A. T. (1967) Photometric error analysis VI. Confirmation of Reiger's theory of scintillation. *Astron. J., 72,* 747–753.